OPEN CHANNEL NOISE

I. Noise in Acetylcholine Receptor Currents Suggests Conformational Fluctuations

F. J. SIGWORTH
Abteilung Membranbiophysik, Max-Planck-Institut für Biophysikalische Chemie, D-3400 Göttingen, Federal Republic of Germany

ABSTRACT The random passage of ions through an open channel is expected to result in shot noise fluctuations in the channel current. The patch-clamp technique now allows fluctuations of this size to be observed in single-channel currents. In the experiments reported here the acetylcholine-induced currents in cultured rat muscle cells were analyzed; fluctuations were found that were considerably larger than expected for shot noise. A low-frequency component, which was fitted with a Lorentzian, was examined in detail; it appears to arise from fluctuations in channel conductance of ~3% on a time scale of 1 ms. The characteristic relaxation time is voltage dependent and temperature dependent ($Q_{10} \simeq 3$) suggesting that the fluctuations arise from conformational fluctuations in the channel protein.

INTRODUCTION

The study of fluctuations in the ionic currents of excitable cell membranes has been widely used to characterize the elementary changes in membrane permeability due to the activity of individual ionic channels. The interpretation of these fluctuations has in recent years been usually based on the assumption that the channels open and close in a discrete fashion, and that the observed current fluctuations result primarily from changes in the number of open channels in the membrane, rather than from fluctuations in the transport of ions through the open channels (see reviews: DeFelice, 1981; Neher and Stevens, 1977). This assumption has generally been verified in the cases where the direct recording of single-channel currents has been made. The purpose of the present study is to investigate the small fluctuations in ion transport that can be observed in single open acetylcholine receptor (AChR) channels.

Fluctuations in the open-channel current are interesting from several points of view. First, because the current is carried by discrete ions, shot noise is expected to be present (Stevens, 1972; Läuger, 1975). This noise is expected to have characteristics that depend on details of the ion permeation process (Frehland and Faulhaber, 1980). Second, current fluctuations might also reflect small fluctuations in the electrostatic or chemical environment of the ions within the channel. In this way the channel pore might be thought of as a preamplifier that allows one to measure very small changes ($\leq 0.01\ kT$) in the energy barriers to ion transport, resulting perhaps from small conformational fluctuations in the protein molecule. Third, it might be possible to gain an insight into the conformational transitions that open and close channels if fluctuations can be observed that precede channel closing or accompany channel opening.

For the present study the AChR channel was chosen because it has been well characterized and because it seemed to have a particularly low open-channel noise level. Other channel types, such as the calcium-activated potassium and nonselective channels (Marty, 1981; Magleby et al., 1982; Colquhoun et al., 1981; Yellen, 1982), show much more prominent noise, which mainly arises from brief channel-closing events; however, this noise would obscure fluctuations of the kind considered here.

The noise observed in the open AChR channel has a relatively large low-frequency (roughly 1 kHz) component and an apparently flat high-frequency asymptote (in measurements to 10 kHz). This paper is concerned mainly with the low-frequency component; the proper analysis of the high-frequency fluctuations will require further characterization of the rapid, poorly-resolved channel-closing events. A preliminary account of this work has already appeared (Sigworth, 1982).

METHODS

Current Recordings

Patch-clamp recordings were made from cell-attached and cell-free membrane patches on cultured rat muscle cells as described in Hamill et al. (1981). Most of the recordings were made on myoballs prepared using a colchicine treatment (Horn and Brodwick, 1980), and used between day 5 and day 14 in culture. Some recordings were also made with myotubes prepared in the same way, but a treatment with cytosine arabinoside (10^{-5}M, 2–3 d) replaced the colchicine treatment.

Solutions with normal and low divalent ion concentrations were used to test for an effect of these ions on the fluctuations (there appeared to be no

Dr. Sigworth's present address is Department of Physiology, School of Medicine, Yale University, 333 Cedar St., New Haven, CT 06510.

effect). The standard bathing solution contained (in millimoles per liter) 140 NaCl, 2.8 KCl, 2 $MgCl_2$, 1 $CaCl_2$, 10 HEPES Na buffer (pH = 7.3); the low Ca^{++} external solution contained 150 NaCl, 0.5 $CaCl_2$ and 0.5 HEPES Na. In some cases the low Ca^{++} solution was additionally buffered by 5 HEPES and 5 histidine, and Na^+ was sometimes replaced by Cs^+. These solutions, with the addition of 0.3–20 μM ACh, were also used in the pipette in the cell-attached and inside-out patch configurations. The internal solutions for cell-free patches contained 150 mM CsCl, 2 mM $MgCl_2$, 0.5 mM HEPES-Na, and 1.1 mM Ca EGTA buffer (pCa $\simeq$ 8) or the same with 0.5 $MgCl_2$ (low Mg^{++} internal solution).

The patch recording techniques were essentially as described in Hamill et al. (1981) except that, during the course of this study, improvements were made in order to decrease the background noise level. In early experiments the pipettes were made from Cee Bee Hematocrit capillaries, and sometimes from Jencons H15/10 Pyrex capillaries. Pipettes made from the latter formed fragile seals that did not allow cell-free recording. In later experiments, Aluminosilicate glass capillaries from AM Systems Inc. (Everett, WA) and from Hilgenberg (Malsfeld, Federal Republic of Germany) were used; these had improved noise characteristics and allowed cell-free recording (Rae and Levis, 1984). Pipette resistances were typically 2–5 MΩ. The pipettes were coated with Sylgard to within 10–20 μm of the tip and heat-polished as described. Inside-out patches were formed by air-exposure of the pipette tip. Outside-out patches were formed by first applying suction to break the membrane under the pipette tip while monitoring the current response to small (~1 mV) voltage pulses. The appearance of large, slow capacitive transients indicated the breakdown of the membrane, and the initial amplitude of the transient was used to estimate the access resistance to the cell interior. Repeated suction was applied if necessary to bring the resistance to a low, stable value (typically 10–30 MΩ) before withdrawing the pipette to form the outside-out membrane. This procedure ensured that the original broken membrane would have a negligible series-resistance effect on the currents through the outside-out membrane.

The pipette current was monitored with an EPC-5 or EPC-7 patch clamp (List Electronic, Darmstadt, Federal Republic of Germany). The frequency compensation of the patch clamp was adjusted to give a step response flat to within 0.5%; the absence of slow-settling artifacts from the recording system was verified by aligning and averaging many channel opening or closing transitions; the resulting time course agreed well with the measured system step response. A Teflon pipette holder was used to reduce the coupling of noise current into the pipette from films of solution inside the holder, and care was taken to keep the holder clean. Best results were obtained by purging the holder with dry nitrogen while pipettes were being changed, in order to keep the interior of the holder dry. The current monitor signal was recorded directly onto FM tape (Racal Store 4 or Store 4 DS; reproduce bandwidth 5 or 10 kHz) at gains chosen to given $\pm$20 or $\pm$10 pA full scale. The latter, higher gain scaling was preferred because the contribution from the flutter-induced tape noise, which depends nonlinearly on the signal amplitude, cannot be removed entirely by the spectral subtraction procedure that was employed.

Signal Analysis

The recorded single-channel currents were subjected to computer analysis of power spectra, amplitude distributions, open-close kinetics, and channel transition time courses. Because the tape-recorded data typically consisted of isolated channel events separated by long gaps, an automatic event-catching program was used (Sigworth, 1983). The tape-recorded signals were filtered by a 4-pole Butterworth filter, and sampled at 2.5 times the filter's cutoff frequency, which was usually 4 or 8 kHz. For the open-close kinetic analysis the tape-recorded data was usually resampled at a rate of 10 kHz following a 4-pole Bessel filter at 2 kHz (−3 dB bandwidth), and analyzed as described. For the calculation of noise amplitude histograms, and for visual inspection of digitized traces, a Gaussian digital filter routine (Colquhoun and Sigworth, 1983) was used to provide variable filtering.

Power Spectra

Individual power spectra were computed using a 16-bit integer fast Fourier transform routine, but were accumulated as double precision (32-bit) integers to avoid round-off errors. The spectra were corrected for the frequency response of the recording system by dividing them point by point by the normalized spectrum of the impulse response of the recording system. The latter was obtained by the following procedure. First, a gated triangle-wave signal was coupled capacitively into the headstage of the patch clamp, and the resulting rectangular current pulses were recorded in the usual fashion. The recorded signals, after filtering, were digitized at two or four times the normal rate and averaged. A single current step from the averaged trace was selected and was differentiated digitally to yield the impulse response, from which the reference power spectrum was computed.

RESULTS

Fig. 1 shows two sets of traces from an outside-out patch with channels activated by 0.3 μM ACh. Although the traces represent successive channel openings in the recording, it is not unlikely that each trace represents the activity of a different channel (two channels in trace 4). The records were digitally filtered to bandwidths of 1 and 4 kHz using a Gaussian filter. At the times when channels are open, narrow spikes are visible that represent brief channel closings, many of which are partial closings to a sublevel of conductance (Hamill and Sakmann, 1981; Auerbach and Sachs, 1983). The existence of a sublevel is suggested by the consistent amplitude of the spikes in trace 4 in the figure and was confirmed by inspection of the records at the full 8 kHz bandwidth. The opening in trace 4 contained an unusually large number of these spikes, and there appeared to be more variability among channel openings in this respect than would be expected from a Poisson process.

Apart from the spikes, a general increase in noise is also observed when a channel is open; this is most clearly seen in the more heavily filtered traces of part B, since the additional noise has a large low-frequency component. The noise appears to be a graded variation in current and does not obviously result from stepwise changes in channel current or from clusters of channel closings. Indeed the amplitude distribution of the open-channel fluctuations (Fig. 2) shows a large increase in variance over the background, but appears to be very nearly Gaussian.

Power Spectrum of the Fluctuations

Since at high frequencies the background noise becomes considerable in amplitude compared to the open-channel noise, average spectra were accumulated from intervals with one channel open and with no channels open, and the latter background spectrum was subtracted from the former. This procedure yields the true spectrum of the channel current fluctuations provided that these fluctuations are not correlated with the background. The properties of the patch recording system, coupled with the fact that the channels were activated at random intervals

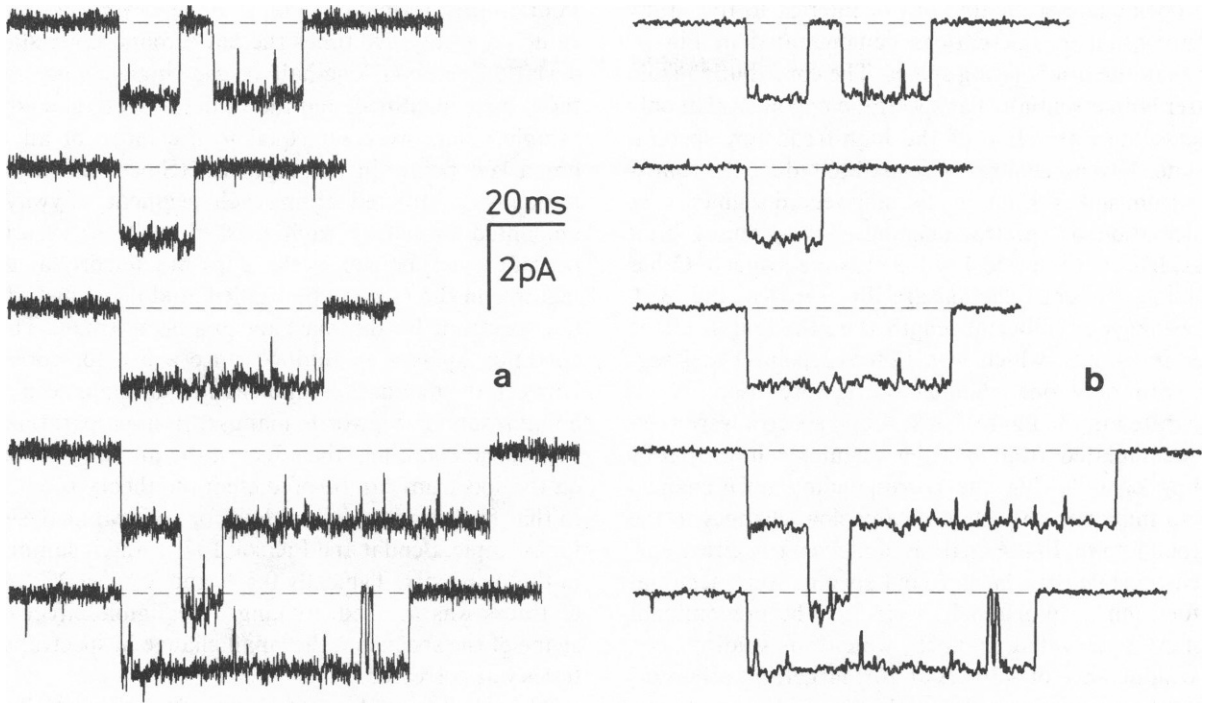

FIGURE 1 Five successive channel events captured by the CATCH program. The recording was from an outside-out patch in low-Ca^{++} external solution containing 0.3 μM ACh; holding potential -100 mV, temperature 9°C. (*a*) The traces are presented after digital filtering with a 4 kHz Gaussian filter; (*b*) the same data but at 1 kHz bandwidth. The time intervals between the beginning of successive traces were 0.12, 0.32, 0.08, and 0.23 s, respectively. Run 45:1920.

by a low concentration of acetylcholine, provides a nearly ideal situation in this respect. The only likely source of correlated fluctuations would be from voltages imposed on the patch, since the patch membrane conductance changes substantially when a channel opens. The voltage fluctuations imposed by the recording amplifier ($S_v \simeq 10^{-17} V^2/Hz$) and the thermal noise of the pipette access resistance ($S_v \simeq 10^{-11}$ V^2/Hz) are, however, quite small: in the worst case of $R_{acc} \simeq 50$ MΩ they induce current spectral densities of roughly 10^{-8} and 10^{-2} times the Johnson noise of the channel itself and can be neglected. Fluctuations in the resting potential of the cells are also expected to be small, and apparently did not contribute significantly to the spectra since similar results were obtained with cell-attached and cell-free patches, as will be seen below.

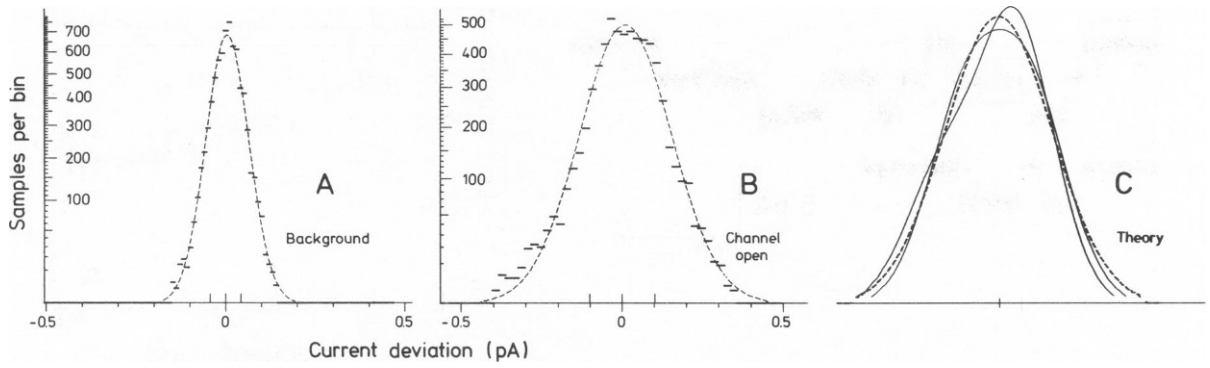

FIGURE 2 Amplitude histograms computed from the same run as in Fig. 1. (*A*) Distribution of the background fluctuations; (*B*) distribution of the fluctuations with one channel open. Record segments were selected as described, digitally filtered at 500 Hz, and masked to remove edge effects and points in the vicinity of brief closures; histograms were then accumulated from the remaining sample points. The dashed curves are Gaussian functions computed to have the same mean, variance, and areas as the experimental distributions. Ordinate values are plotted according to a nonlinear (square-root) transformation that stabilizes the variance, causing the expected (Poisson) statistical errors to appear constant in size. *C*, a comparison of the Gaussian distribution (dashed curve) with distributions computed on the basis of fluctuations between two closely spaced current levels (see Discussion) with $r = 1$ and the level spacing $j = 0.20$ pA (symmetrical curve) and with $r = 3$, $j = 0.33$ pA (skewed curve).

The open-channel fluctuations of interest to this study are the continuous fluctuations demonstrated in Fig. 1, rather than the brief closing spikes. The contribution from the latter is an essentially flat spectral component that only confounds the estimation of the high-frequency spectral amplitude. Two procedures were used to reduce the contributions from spikes. First, in choosing record segments for the calculation of spectra, openings having many brief closings, like that in trace 4 of Fig. 1, were avoided. Other criteria for segment selection are illustrated in Fig. 3 *A*. Only openings of sufficient length (i.e., the length of the Fourier transform, which was 128–512 points) and segments with only one channel open were used. As is demonstrated in the figure, background spectra were typically accumulated from baseline segments immediately preceding or following the corresponding open-channel events to minimize the effect of any slow changes in the background noise. In the analysis of a given run either one, or when possible, two background spectra were accumulated for each open-channel spectrum. The predominant class of ACh-activated channels, which was studied here, had a conductance of ~30 pS at 20°; larger, 50 pS events with shorter open times, probably from junctional type channels (Hamill and Sakmann, 1981) were occasionally observed. Their open times were too short to allow spectral analysis.

A second procedure for reducing the spectral contribution from spikes was to mask them from the record before Fourier transformation. Points lying beyond a threshold value (typically five times the background noise standard deviation or about one-half of the single-channel amplitude) were identified, and the values of these and adjacent sample points were set equal to the mean of all of the unmasked points in the segment. (Since the mean was normally subtracted from each segment anyway, this amounted to setting each masked point to zero.) This procedure is justified if the gaps are uncorrelated with features in the noise to be studied, and if the distortion of the spectrum by the masking process is small. The first condition appears to fulfilled since a test for correlation between the fluctuations and channel gating is seen to give a null result (F. Sigworth, manuscript in preparation). For the second condition, the effect of the masking procedures on the spectrum can be predicted; the theory is analogous to that for "windowing" of data for spectral analysis (see, for example, Bendat and Piersol, 1971), and is summarized in the Appendix. Typically 0.5%, and at most 2%, of a set of traces was masked, making a negligible effect on the shape of the spectrum; the small change in spectral amplitudes was corrected.

The selection and masking procedures do not eliminate all brief closing events, so that an excess flat spectral component is expected to be present in the spectrum. The size of this component can be estimated by analyzing the amplitude distribution of the fluctuations; this procedure will be described in a subsequent paper.

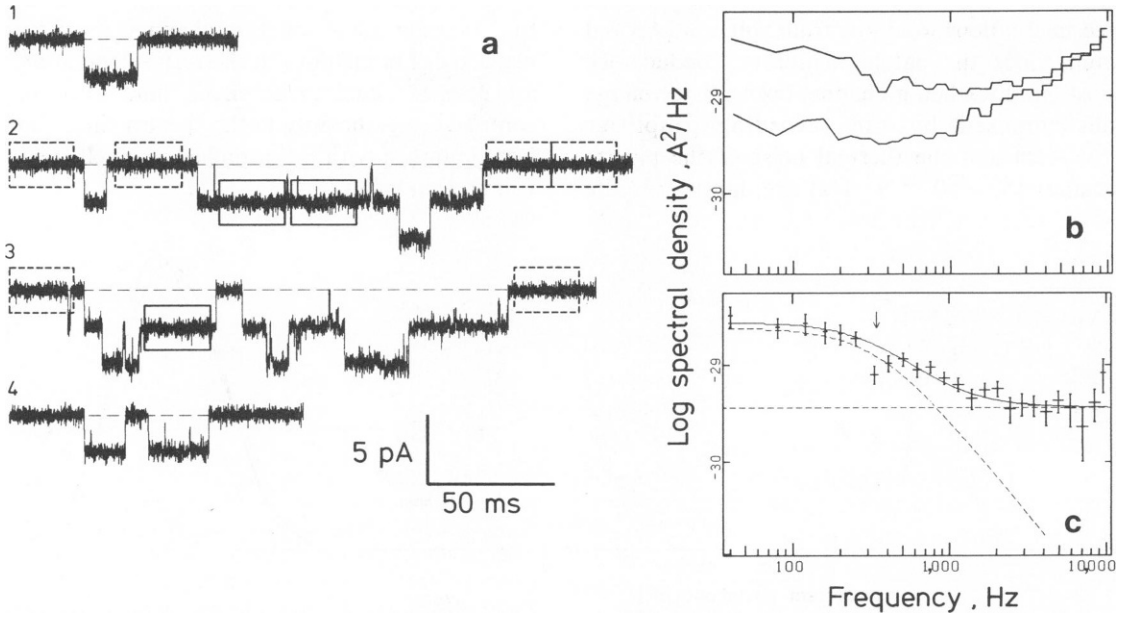

FIGURE 3 Selection of record segments and calculation of spectra. (*a*) Original traces are shown at the full 8 kHz bandwidth; dashed boxes indicate segments (512 points at 50 μs/point) that were selected for the background calculation, and solid boxes enclose open-channel segments. The box heights represent the masking threshold, in this case ±1.6 pA, so that points extending outside of the boxes were masked. In trace *1*, the channel opening was too short, and so was excluded: overlapping events in traces *2* and *3* were also excluded. (*b*) Averaged spectra from 23 channel-open segments (*upper* curve) and adjacent background segments (*lower* trace) are shown. In *c* the spectral differences are plotted with error bars indicating ±1 SE, calculated assuming independent, chi-square distributed spectral estimates as would be expected from random phases in the original fluctuations. The dashed curves show the Lorentzian and constant components that are summed (solid curve) to fit the points. Run 45:1920.

Fig. 3 *B* shows average spectra computed from channel-open and background segments selected and processed in this manner. A comparison of the two curves shows that the opening of a channel causes a large (roughly sixfold) increase in the spectral density at or below 300 Hz. The change at higher frequencies is less distinct due to the increase of the background noise density with frequency. The corresponding difference spectrum is shown as part *C* of the figure. The error bars in this and succeeding spectral plots represent ±1 SE, computed on the basis of the usual assumption that individual spectral estimates are independent and chi-square distributed. Spectral estimates at high frequencies are relatively uncertain because they are obtained as a small difference between two large numbers; this is the primary limitation on the frequency range over which spectra could be evaluated.

The difference spectra generally showed flat low- and high-frequency asymptotes, with a transition between the two levels in the general vicinity of 1 kHz. Because of the flat asymptotes the spectra could not be acceptably fitted by a power law function (e.g., a $1/f$-type spectrum) but could be fitted with the sum of a Lorentzian function and a constant

$$S(f) = \frac{S_0}{1 + (f/f_c)^2} + S_1.$$

The two terms in the fitting function are illustrated by the dashed curves in Fig. 2 *C*. This function is appealing because of its possible physical significance: the Lorentzian would represent a relaxation process whose characteristic time constant τ is related to the corner frequency f_c by $\tau = 1/(2\pi f_c)$, and the constant component would arise from one or more rapid processes, such as shot noise, rapid conductance fluctuations, or unresolved gaps, whose dispersions would be beyond the accessible frequency range. In this study it was assumed that the two components result from disparate, independent processes, implying that they can be studied separately.

In the spectrum of Fig. 3 *C*, the fitted slow (Lorentzian) component had a corner frequency f_c of 350 Hz, corresponding to a relaxation time of ~0.5 ms, and the low-frequency spectral amplitude $S_0 = 2.36 \times 10^{-29}$ A²/Hz. The root mean square (rms) current fluctuation resulting from this component, normalized by the single channel current ($i = 2.6$ pA in this case) is given by

$$\sigma = \sqrt{\frac{\pi S_0 f_c}{2i^2}} \qquad (1)$$

and was equal to 0.027. The fast (i.e., constant) spectral component had a spectral density $S_1 = 3.7 \times 10^{-30}$ A²/Hz, some 3.8 times the spectral density $S = 2iq$ expected for shot noise in the current i from independently transported ions with a charge q equal to the elementary charge.

Effects of Temperature and Patch Configuration

The apparent corner frequency of the slow component is temperature dependent as is demonstrated in Fig. 4 *A* and *B*. The spectra were obtained from the same patch at temperatures of 9 and 19°C, respectively. With the temperature change the corner frequency of the slow component increases by a factor of 2.4, while the relative size σ of the fluctuations changed little. The values of the corner frequency and the amplitude of the high-frequency component varied considerably from patch to patch; Fig. 4 *C* shows the channel open-time distribution and spectrum from a different patch at 14°C. This patch showed a higher f_0 value than the other one at 19°C, even though the channel open time was longer.

Trends in the temperature dependence of the noise parameters are observed when the results from a number

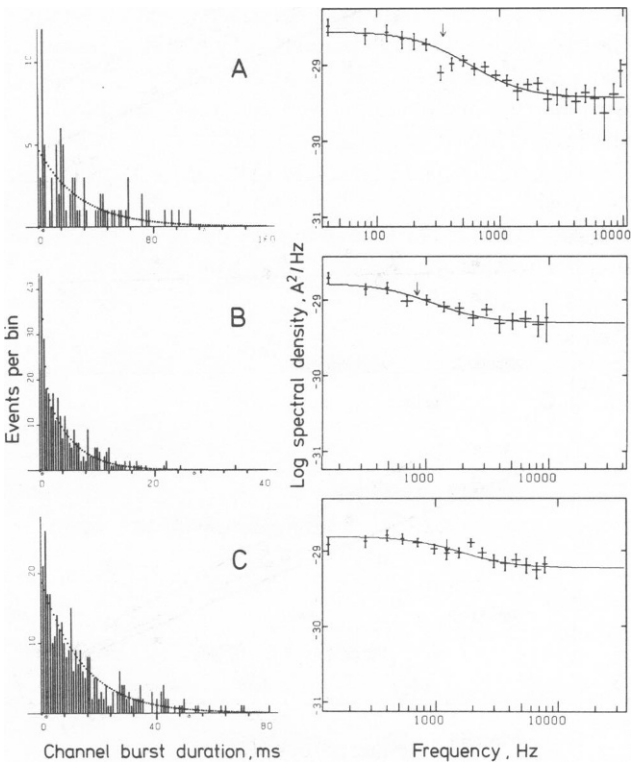

FIGURE 4 Temperature dependence on channel open times and open-channel noise spectra. *A* is from the same run as in Figs. 1–3 at 9°C, τ_b = 29 ms. f_c = 350 Hz (0.45 ms): *B* is from the same outside-out patch but at 19°C, −100 mV holding potential τ_b = 0.4, 4.7 ms. f_c = 850 Hz (0.19 ms.). *C* is from a different, cell-attached patch held 40 mV hyperpolarized (estimated absolute potential −100 mV) at 14°C in the presence of 1 μM ACh; τ_b = 14.2 ms. f_c = 1,250 Hz (0.13 ms); run 26:720. For the histograms the channel open times were estimated as burst durations (Sigworth, 1983) using critical gap durations of 1 ms for recordings made below 12°C, as in *A*, 0.7 ms for temperatures to 18°C, and 0.5 ms for higher temperatures. All three histograms show an excess of short events; this is most obvious in *B*, which, because of the good statistics, allowed two exponential components to be fitted. Where this was not possible, the first bins were ignored in the fits. The single-channel currents were −2.7, −4.5, and −3.1 pA, respectively.

of experiments are pooled (Fig. 5). The relaxation times τ, relative amplitudes σ and the mean channel open (burst) durations τ_b are plotted as a function of temperature; The corner frequency estimates show a large scatter but the decrease with temperature (Q_{10} of ~3) is similar to the change in channel open time, keeping the ratio τ/τ_b approximately constant at 0.02. The relative fluctuation amplitude σ remains constant at ~3% independent of temperature.

The scatter in values of τ and τ_b is larger than can be expected from uncertainties in the fitting process and appears to arise from a substantial variation in channel properties between batches and cells and even between patches from a single cell. In some patches the kinetic analysis showed multiple components in the burst duration histograms, as in Fig. 4 *B*, suggesting an inhomogeneity in channel characteristics as has been observed by Jackson et al. (1983). The variations in τ, however, did not correlate well with variations in τ_b, suggesting that these parameters are not closely related. A considerable fraction (roughly 20%) of the patches studied had only short-lived channel events that were too brief to allow spectral analysis; their parameters are not shown in the figure.

The various symbols in Fig. 5 indicate different patch configurations and solutions. No consistent differences in fluctuations were observed among the three patch-recording configurations (cell-attached, inside-out and outside-out) and between solutions with normal or reduced concentrations of divalent ions and pH buffer.

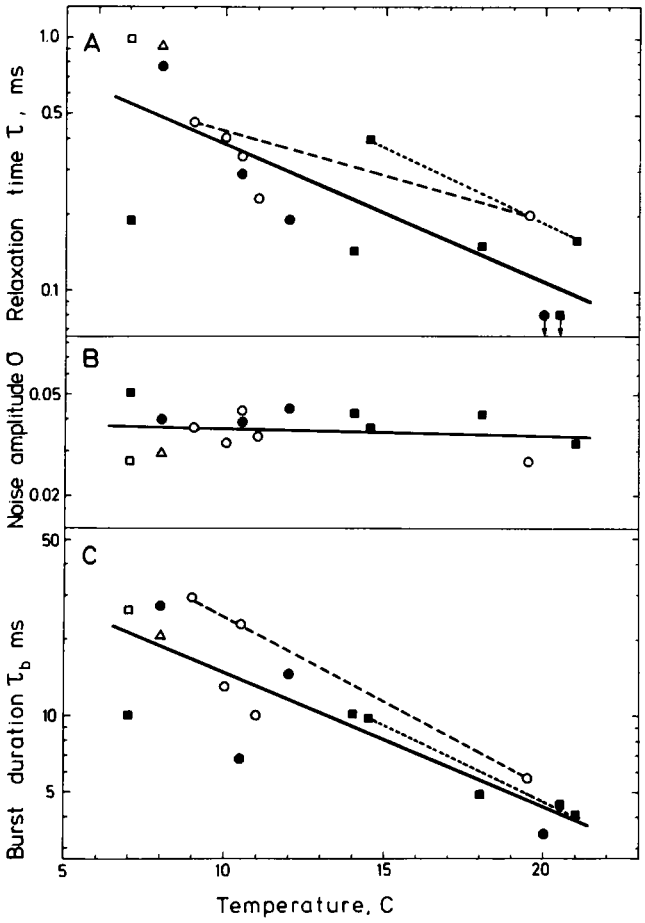

FIGURE 5 Temperature dependence of parameters, pooled from 17 runs on 15 patches. (*A*) Relaxation times computed from the corner frequency of the fitted Lorentzian function; (*B*) rms fluctuations amplitude, normalized by the channel current, calculated according to Eq. 1; (*C*) channel open time, determined from fits to histograms of burst durations as in the preceding figure; in cases where two components were resolved, the longer time constant is plotted. Dashed lines connect values obtained from the same patch at different temperatures; solid lines indicate least-square fits yielding Q_{10} values of 3.4 in *A*, 1.07 in *B*, and 3.4 in *C*. The various symbols identify patch configurations and recording conditions: ○ and □ are from outside-out patches in low- and normal-Ca^{++} solutions, respectively; △ is from an inside-out patch in normal solution: ● and ■ are from cell-attached patches in low and normal-Ca^{++} solutions. The cell-attached recordings at 10.5°C and at 14.5°C were from myotubes that were not treated with colchicine.

Effects of Other Conditions

As the single-channel current was increased by hyperpolarizing the patch membrane, the variance of the fluctuations also increased, nearly as the mean current squared (Fig. 6). A quadratic relationship would in fact be expected if the slow fluctuations arose simply from a modulation of the channel conductance. Since the fluctuations would likely arise from the motion of one part of the channel, affecting for example, the affinity of an ion binding site, they would, in general, affect the conductance in a voltage-dependent manner. This could give rise to the observed slopes that are <2.

There was a tendency for f_c to increase with hyperpolarization, with change of *e*-fold in ~40 mV. Fig. 7 shows spectra from one outside-out patch in the range of −70 to −120 mV. Potentials outside this range were not studied: below −70 mV the currents are smaller relative to the background noise, making brief closures harder to identify,

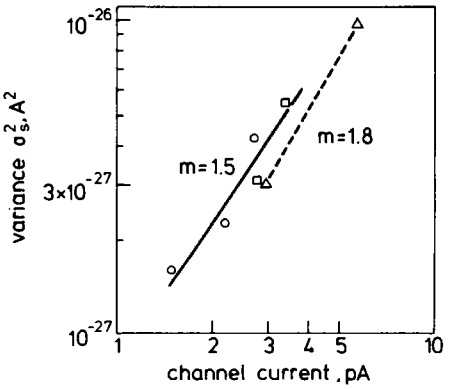

FIGURE 6 The absolute variance σ_s of the slow component, computed as $(\pi/2)S_* f_c$ and plotted as a function of the single-channel current. Currents were varied by changing the potential and permeant ions; ○ and □ are from the same outside-out patch with Na^+ (−70 to −120 mV) and Cs^+ (−100 to −120 mV) respectively; △ are from a cell-attached patch in Cs^+ (−50 and −130 mV relative to rest).

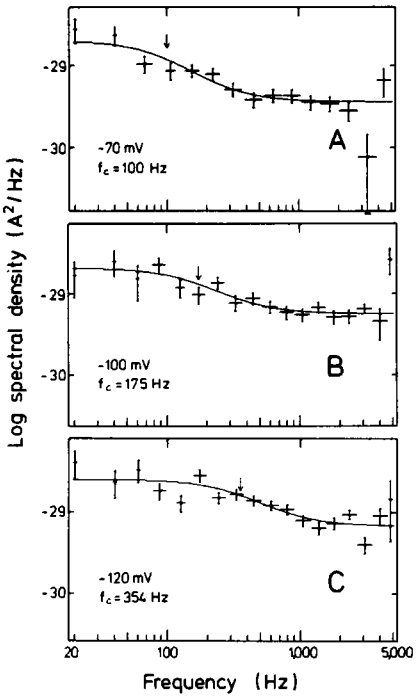

FIGURE 7 Open-channel noise spectra obtained at three membrane potentials. Recordings are from an outside-out patch at 7°C in normal Ca^{++}, 1 μM ACh. The corresponding single-channel currents were −1.5, −2.2, and −3.3 pA at −70, −100, −120 mV; the mean channel open times were 30, 37, and 44 ms. Runs 7:700–980.

while beyond −120-mV seal breakdown starts to occur in cell-free patches. Positive membrane potentials were also not examined because the short channel lifetime and many brief interruptions in the currents precluded spectral analysis.

Substitution of Cs^+ for Na^+ as the permeant ion increased i by a factor of 1.3 (see also Hamill, 1980) and resulted in somewhat smaller values of σ. In four experiments the values of σ were in the range 0.020 to 0.024, lower than any seen with Na^+ (Fig. 5 *B*).

In a few runs the permeant ion concentration was changed. In one experiment sucrose was added to maintain osmolarity as the Cs^+ concentration was reduced to 30 mM, while in another experiment osmolarity was allowed to vary as the Na^+ concentration was varied from 250 to 72 mM. In both cases the roughly fourfold reductions in concentration resulted in increases in σ by a factor of ~1.5; that is, the absolute variance of the fluctuations remained approximately constant while the single-channel currents decreased by this factor. The small decrease in current presumably reflects the saturation of the channel conductance (Horn and Patlak, 1980). It is not clear, however, whether this effect of ion concentration is a specific effect of the permeating ion or simply related to the ionic strength.

Most experiments were performed using ACh concentrations in the range of 0.3 to 2 μM. In a few cases, however, 20 μM ACh was applied; this resulted in strong bursting behavior, presumably due to desensitization kinetics (Sakmann et al., 1980); a typical recording from a myoball at this concentration is illustrated in Sigworth (1983). An increase, approximately a doubling, of the high-frequency spectral amplitude was usually observed at 20 μM ACh. Such an increase might be expected from an increased frequency of gaps due to the blockage of the channel by ACh (Sine and Steinbach, 1984).

Treatment with concanavalin A (Con A) has been shown to inhibit the lateral diffusion of ACh receptors (Axelrod et al., 1978). In an attempt to test for a possible connection between lateral diffusion and current fluctuations, cells were treated with 1 mg/ml Con A in the standard external solution for 1 h at 37°C. After treatment no ACh-receptor currents could be recognized in patch recordings, even though (as a check for an intact membrane and correct recording conditions) Na^+ channel currents were sometimes observed, and cell resting potentials remained near −60 mV.

DISCUSSION

When compared with the open-close gating of channels, the observed fluctuations in open-channel currents are quite small. Fig. 8 compares the spectrum expected from the gating of the channels shown in Figs. 1 and 3 with the open-channel noise spectrum; the low-frequency asymptotes differ by more than four orders of magnitude, and the open-channel noise would be completely undetectable in conventional measurements of ACh-induced noise. Note, however, that above ~2 kHz the open-channel noise would be expected to dominate the spectrum.

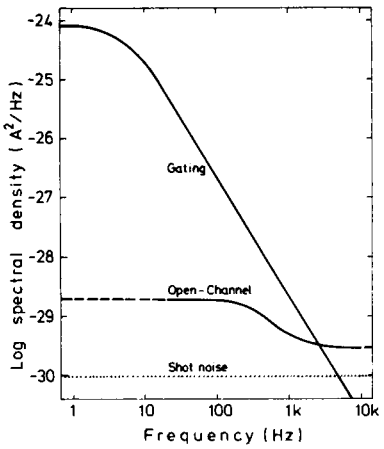

FIGURE 8 A sketch of the relative amplitudes of the expected open-closed gating noise, open-channel nosie and shot noise in an AChR channel with parameters corresponding to the run depicted in Figs. 1–3. The spectral amplitudes are proportional to the average number of open channels Np; this was chosen to be equal to 1 for comparison with the open-channel noise spectrum. The corner frequency of the gating noise spectrum was 5.5 Hz, chosen to correspond to the 29-ms burst duration. (The minor gating-noise component due to brief gaps is not shown.) The dotted line showing the expected shot noise level is computed according to Schottky's formula, $S(f) = 2iq$, with i = 2.6 pA.

The open-channel current fluctuations are surprisingly large when compared with the expected shot noise level, indicated by the dotted line in Fig. 8. The excess fluctuations at high frequencies most probably arise from very rapid interruptions in the channel current; the low-frequency fluctuations, on the other hand, do not arise from interruptions of the current but instead appear to be from small changes in the channel conductance. Note that the low-frequency part of the spectrum appears to have a flat asymptote and does not show $1/f$ behavior. A spectrum of the latter form, in which the spectral density decreases steadily as the inverse of frequency, has been observed in a number of systems where current is carried by a limited number of charge carriers (Hooge, 1976) and has also been reported in measurements of noise in certain excitable membranes (see Neumcke, 1978 and 1982 for reviews); it has generally not been seen in ACh-activated currents. That $1/f$ noise might arise from a mechanism in single open channels is implied by the results of Sauve and Bamberg (1978) who observed such a spectrum in the current carried by permanently-open gramicidin A channels; however, the spectral density that they observed, when scaled according to the assumption that channels are independent $1/f$-noise sources, is much larger than that observed here.

Auerbach and Sachs (1984) have reported fluctuations similar to those seen here in ACh receptors of chick muscle. Interpreting their cumulative spectrum as a Lorentzian one obtains $f_c \simeq 2$ kHz and $\sigma \simeq 0.05$ for an experiment at room temperature, values similar to those obtained here. They also measured the fluctuations in the current in the subconductance state and found them to have an even larger variance. In rat myoballs a noisy subconductance state is also seen (Hamill and Sakmann, 1981), but its properties were not studied.

Does the Channel Switch between Two Levels of Conductance?

One explanation for the apparently Lorentzian low-frequency component of the fluctuations would be that the open channel shows stepwise transitions between closely spaced conductance levels, say i_1 and i_2 as in the scheme

$$i_1 \underset{k_{12}}{\overset{k_{21}}{\rightleftharpoons}} i_2. \tag{2}$$

The measured relative magnitude σ and corner frequency f_0 of the Lorentzian part of the spectrum are sufficient, with the addition of one further parameter, to constrain the values of the rate constants k_{12} and k_{21} and the spacing of the current levels. Let the free parameter be $r = k_{12}/k_{21}$, the ratio of the mean dwell times at the two levels, and define $j = i_1 - i_2$, the spacing of the current levels. Then the model parameters are given by

$$\begin{aligned} k_{12} &= 2\pi f_0 r/(1 + r) \\ k_{21} &= 2\pi f_0/(1 + r) \\ j &= \sigma i(1 + r)/r^{1/2}. \end{aligned} \tag{3}$$

Choosing $r = 1$, the value for which j takes its minimum value of $2\,i\sigma$, along with the parameters $f_0 = 349$ and $i\sigma = 0.144$ pA from the spectrum in Fig. 4 *A*, the values become $k_{12} = k_{21} = 110\ s^{-1}$ and $j = 0.203$ pA. Steplike transitions of this size are, unfortunately, not quite recognizable in simulated records when background and high-frequency noise components are added.

A test for stepwise current changes of this kind can be made by comparing the experimental amplitude distribution of the fluctuations with the predictions of this theory. In the absence of background noise the distribution from the switching process is distinctly non-Gaussian, and should in fact have two peaks when the effective recording bandwidth is sufficiently large (FitzHugh, 1983; Yellen, 1984). The effect of other noise sources is to smear out this distribution, however, so that the result differs only slightly from Gaussian. Fig. 2 *C* shows the distributions expected from the switching process with $r = 1$ and $r = 3$. The current steps were taken to be filtered with a 500-Hz Gaussian filter and the total variance of the other (background and high-frequency component) noise sources was computed to correspond to the experimental distribution in Fig. 2 *B*; the other noise sources were assumed to be Gaussian distributed. For $r = 1$ the switching distribution has a lower peak and slightly broader sides than the Gaussian (shown as a dotted curve). For $r = 3$ the distribution is clearly skewed. The experimental distribution also differs from Gaussian, but not in the form expected from the switching mechanism; the peak is not depressed or skewed, and the tail that is observed cannot be fitted well by varying r. From this analysis it therefore appears likely that the fluctuations do not arise from a simple two-level switching mechanism. The remaining possibilities include a continuous, random change in channel current, or discrete transitions among three or more levels. Two-level transitions of variable size, for example from individual channels having different characteristics, could also result in the more nearly Gaussian distribution that is observed.

There did appear to be a small variation in the average channel conductance from one event to the next. For example, in the run of Fig. 7 *B* the average channel currents during the intervals, used for accumulating spectra (duration $T = 51$ ms) were 2.16 ± 0.055 pA (SD; $n = 19$). Part of the variation can be explained by the fluctuations themselves. Assuming that the spectral density has a constant value S_0 below the lowest measured spectral point (at 20 Hz), the expected standard deviation would be $(TS_0)^{1/2} = 0.02$ pA in this case. The remaining variation could be due either to slow fluctuation processes or to small

variations among individual channels, since each opening event is likely to reflect a separate channel.

Fluctuations from Diffusion Processes?

The process of ion permeation itself is too rapid to explain the slow fluctuations that are observed in the open-channel current. The channel current of a few picoamperes corresponds to the transport of more than 10^7 ions per second; since it is likely that at most only a few ions are in the channel at any one time, any fluctuations due to transport through the channel would be on the time scale of 1 μs or less. The transport of ions from the bulk solution to the channel would also not be expected to show slow fluctuations, since interactions between ions are limited to distances on the order of a Debye length (~10 Å), whereas the diffusion of ions is so rapid that interaction lengths on the order of 1 μm to would be required to yield fluctuations that occur on a millisecond time scale.

Fluctuations having appropriately long time scales could conceivably result from diffusion processes that affect the environment of the channel, for example the electrostatic potential in the channel, in a way to influence the ion flux. Diffusion of ions in the aqueous phases is again too rapid to produce such fluctuations, but diffusion in the membrane can occur on an appropriate time scale. Weissman (1978) has proposed a theory in which the interactions among diffusing channels result in $1/f$ noise; this mechanism does not apply to fluctuations in a single channel, but the idea to be considered here is similar. Suppose that there are diffusing, charged molecules present in the membrane which, when they are within a characteristic distance r_0 from the channel, have an effect on the channel current. The spectrum of current fluctuations would then be expected to show some sort of feature in the vicinity of the frequency $f_0 = D'/2\pi r_0^2$ where D' is the sum of the lateral diffusion coefficients of the AChR protein and the interacting molecule. Choosing for example $D' = 10^{-9}$ cm^2/s, a typical value for the diffusion of a small protein, and $r_0 =$ 50 Å, a reasonable scale length for electrostatic interactions within the membrane, one obtains $f_0 \simeq 1$ kHz.

A diffusion mechanism for the observed fluctuations is nevertheless unlikely for three reasons. First, the apparent relaxation time of the fluctuations is quite temperature dependent, with a Q_{10} value near 3 (see Fig. 5). The temperature dependence of diffusion constants for AChRs and lipids, measured also in cultured rat muscle by Axelrod et al. (1978), is, however, only weakly temperature dependent, with $Q_{10} \lesssim 1.5$. Second, the observed relaxation time is significally dependent on membrane potential (Fig. 6), whereas lateral diffusion would not be expected to be potential dependent.

The third problem with the diffusion mechanism is that the form of the expected spectrum provides a poor fit to the experimental spectra. Fig. 9 shows spectra predicted on the basis of a particular functional form for the interaction between the diffusing molecules and the channel; the general features of this spectrum are expected to be common to most physically reasonable interaction functions. The channel current i is assumed to vary with the distance r between the channel and an interacting molecule according to

$$i = i_0 + w(\mathbf{r}), \tag{4}$$

where the interaction function was chosen to be

$$w(\mathbf{r}) = w_0 \exp(-|\mathbf{r}|^2/2r_0^2), \tag{5}$$

to allow a closed form expression to be obtained for the temporal autocovariance function

$$\begin{aligned} C(\tau) &= \langle i(0)\, i(\tau)\rangle - i_0^2. \\ &= s_i \int\int w(\mathbf{r})w(\mathbf{r}')p(\mathbf{r}', \tau; \mathbf{r})\mathrm{d}^2\mathbf{r}\mathrm{d}^2\mathbf{r}'. \end{aligned} \tag{6}$$

The integrals are taken over the membrane area (assumed here to be infinite); s_i is the concentration of diffusing particles and the function p is a solution of the diffusion equation that gives the probability density of the particle being at $\mathbf{r}'$ at time τ given that it is at $\mathbf{r}$ at time zero. The autocovariance function is exactly the same as that arising in fluorescence correlation spectroscopy of a two-dimensional system (Fahey et al., 1977) and is evaluated to yield

$$C(\tau) = \frac{\sigma_0^2 i^2}{1 + D'\tau/r_0^2}, \tag{7}$$

where the variance $\sigma_0^2 = \pi s_i r_0^2 w_0^2$. The resulting power spectrum, obtained as the Fourier transform of C, is

$$S(f) = \frac{2\sigma_0^2 r_0^2}{D'}\,[-\mathrm{Ci}(\nu)\cos(\nu) - \mathrm{si}(\nu)\sin(\nu)], \tag{8}$$

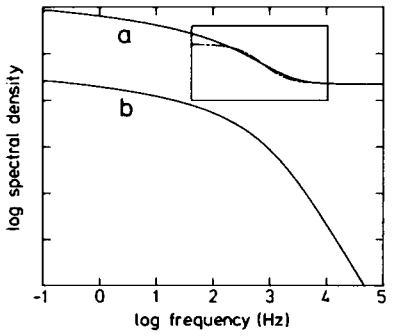

FIGURE 9 The spectrum predicted from a theory involving lateral diffusion of particles that interact with the channel. Curve *a* shows the sum of the diffusion noise plus a constant component, while *b* shows the diffusion noise alone, given by Eq. 10. The inset shows the fitting function from Fig. 4 *A* (dashed curve) and indicates the limited frequency range (40 Hz to 10 kHz) over which the experimental data extend. The diffusion noise spectrum was computed from the parameters $D' = 1.04 \times 10^{-9}$ cm^2/s and $r_0 = 50$ Å.

where the reduced frequency ν is given by

$$\nu = 2\pi r_0^2 f/D.$$

At low frequencies the asymptotic behavior of $S(f)$ is proportional to $\ln(f)$, while the high frequency asymptote is $1/f^2$. As can be seen from the plot of this function (curve *b* in Fig. 9), the transition between these regimes is very gradual compared to a Lorentzian function, and occurs over several decades in frequency. Curve *a* compares this function, with a constant component added, to the function fitted to the experimental spectrum in Fig. 4 *A*. The box indicates the range of experimentally accessible frequency values, and the dashed curve shows the Lorentzian-plus-constant fitting function that was used in Fig. 4 *A*. As can be seen, the gradual rolloff of the function (8) makes it impossible to obtain a relatively flat low-frequency asymptote while obtaining a rapid decrease in spectral density in the intermediate frequency range. Although this function is based on the particular form (Eq. 5) assumed for the interaction function $w(r)$, the two-dimensional diffusion process will always result in logarithmic low-frequency behavior of the spectrum regardless of the specific choice of w. Further, more realistic interaction functions, which, for example, include a $1/r$ dependence of w at small r, will result in even more gradual rolloff at high frequencies. Thus, it appears that this mechanism cannot explain the observed fluctuation spectrum.

Another possible source of fluctuations would be the exchange of lipid molecules tightly bound to the channel protein. Typical rates of exchange have been estimated to be in the range 10^6–10^7 s^{-1} on the basis of electron spin resonance measurements (Marsh et al., 1981), which would be too rapid to explain the observed spectrum.

Conformational Fluctuations of the Channel Protein

The most likely explanation for the slow fluctuations is the presence of conformational fluctuations within the channel protein that have an effect on the channel conductance. In favor of this possibility are the observed temperature dependence and voltage dependence of the spectrum of the fluctuations. The Q_{10} value of ~3 is similar to that for the channel-gating process in the AChR itself as well as in other channel proteins. The voltage dependence of the fluctuation time constant, roughly *e*-fold in 40 mV, is similar in magnitude (but opposite in sense) to that of the channel open time, and requires that the motion that gives rise to the fluctuations be coupled to a substantial charge movement, equivalent to at least 0.8 elementary charges acting through the membrane potential.

Internal motions in proteins are known to occur on a wide range of time scales (Careri et al., 1975) and have been studied by a variety of techniques including computer modeling, nuclear magnetic resonance (NMR), solvent exchange, x-ray diffraction and ligand-binding kinetics (Karplus and McCammon, 1981; Gurd and Rothgeb, 1979; Debrunner and Frauenfelder, 1982). On the time scale corresponding to the slow fluctuations observed in the present study, the main source of information about structural fluctuations comes from NMR measurements. For example, Wagner et al. (1976) have analyzed proton NMR spectra to study the rotational mobility of the eight aromatic side chains in the pancreatic trypsin inhibitor molecule. Changes with temperature of the line shapes and patterns from four of the aromatic rings were consistent with 180° ring flips occurring on time scales of 10^{-4} to 10^{-1} s, with activation enthalpies for the process of roughly 14 kcal/mol. The actual flipping of a ring occurs in ~10^{-12} s (McCammon and Karplus, 1980); the slow kinetics observed in the NMR experiments arise from the dwell times in each of two metastable configurations.

Two-state fluctuations that may arise from a similar mechanism have been reported in chemically modified gramicidin A channels (Szabo, 1981) were interruptions in current flow on a millisecond time scale apparently result from the sterically hindered rotation of several residues. The activation enthalpies for the two rate constants of the blocking process were found to be 14.5 and 19.8 kcal/mol. This sort of mechanism, in which conformational transitions occur rapidly but relatively rarely, can explain the slow kinetics and the temperature dependence of the observed AChR current fluctuations as well; the observed Q_{10} value near 3 corresponds to an activation enthalpy of ~18 kcal/mol. As we have seen, however, a test for two-state behavior of the fluctuations had a negative result. A slightly more complicated behavior, for example having three levels or more than one site of motion, could explain the observed distribution of fluctuation amplitudes. The relatively low amplitude of the fluctuations, roughly 3%, can also be explained on the basis of the large size of the AChR, with the conformational changes far removed from the channel itself.

APPENDIX

Effect of Masking on the Power Spectrum

A masking procedure was used to remove large spikes from data segments before computing the power spectrum. These spikes (Fig. 10 *A*) arose in open-channel segments due to brief channel closings. They were removed by means of a masking function $m(t)$ that was zero at times when the data segment exceeded a threshold level and at the adjacent sample points, but unity otherwise. In an iterative procedure, the original data segment $x_0(t)$ was multiplied by its mask $m_0(t)$ to yield the masked trace $y_0(t)$; the mean value of y_0 was then calculated and subtracted from x_0 to yield the baseline-shifted version $x_1(t)$ and the process was repeated until the mean of the masked trace was zero. This procedure ensured that the masked points were set to the mean of all other points in the trace (i.e., zero) and that the thresholds for masking were symmetrically placed.

The effect of masking on the power spectrum can be readily estimated if the assumption is made that the spikes are uncorrelated with the other fluctuations in the data segment. Let $x(t)$ be a zero-mean, stationary random process representing the fluctuations of interest in the original

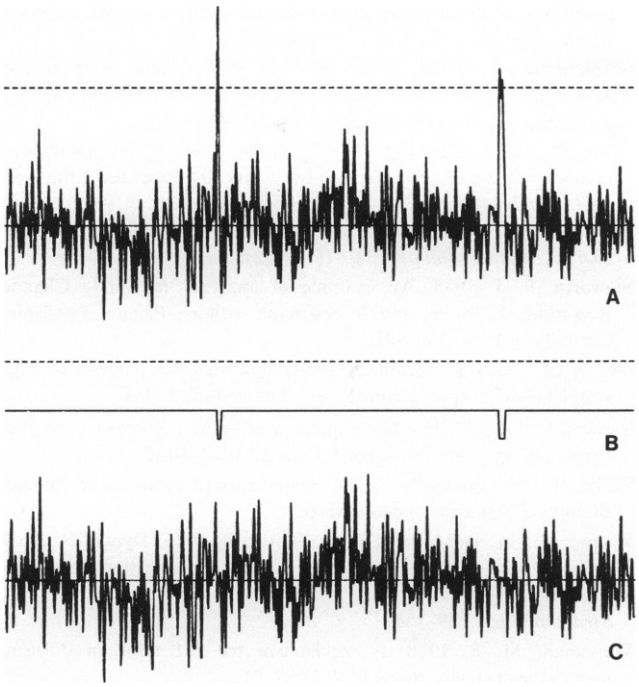

FIGURE 10 Demonstration of masking. (*A*) a 512-point data segment is shown; the dashed lines indicate the ±1.6 pA thresholds for masking. (*B*) the masking function $m(t)$, which is zero for intervals of three and five sample points, and unity otherwise. (*C*) the data segment after masking. Sample intervals 50 μs; same recording as in Fig. 3. The traces in *A* and *C* were cubic-spline interpolated (Colquhoun and Sigworth, 1983) for plotting.

record but containing no spikes, and let $m(t)$ be a binary, stationary random process representing the masking function. The masked process

$$y(t) = m(t)x(t) \qquad \text{(A1)}$$

has the autocorrelation function given as the ensemble average

$$R_y(\tau) = \langle m(0)x(0)m(\tau)x(\tau)\rangle,$$

which can be evaluated explicitly as

$$R_y(\tau) = \int\int\int\int m_0 x_0 m_\tau x_\tau f(m_0, x_0, m_\tau, x_\tau)\, dm_0 dx_0 dm_\tau dx_\tau, \qquad \text{(A2)}$$

where m_0, x_0, etc., are realizations of the processes m and x at times 0 and τ, and $f(m_0, x_0, m_\tau, x_\tau)$ is the joint probability density of these realizations. Since x and m are independent, we can write f as a product

$$f(m_0, x_0, m_\tau, x_\tau) = [f_m(m_0, m_\tau)][f_x(x_0, x_\tau)]$$

of two density functions f_m and f_x, allowing the integral to be separated to yield

$$R_y(\tau) = \langle m(0)m(\tau)\rangle \langle x(0)x(\tau)\rangle = R_m(\tau)\, R_x(\tau). \qquad \text{(A3)}$$

the product of the autocorrelations of m and x.

The power spectrum $S_y(f)$ of y will then, by the convolution theorem, be given by the convolution of the spectrum of x with the spectrum $S_m(f)$ of m. As an example of $S_m(f)$ consider $m(t)$ to be unity except for occasional intervals of fixed duration w when it is zero; these intervals occur at random (Poisson process) with frequency λ. We assume further that the frequency is very low, so that the effects of overlapping intervals can be neglected. The probability of masking is then

$$p = \lambda w,$$

and the spectrum is

$$S_m(f) = (1 - p)^2\delta(f) + p(1 - p)w\left[\frac{\sin(wf)}{wf}\right]^2, \qquad \text{(A4)}$$

which consists of a delta function having nearly unity area, and side lobes having an area of $\sim p$. The small size of the side lobes ($p \leq 0.02$ here) results in a negligibly small distortion of the form of the spectrum. Therefore the only correction that was made for the masking process was to scale the resulting spectrum $S_y(f)$ by the factor $(1 - p)^{-1}$ to correct for the reduction in the total area.

I wish to thank Dr. E. Neher for his encouragement, Dr. O. P. Hamill, with whom some early experiments were done, and H. Karsten and M. Pilot for preparing the cells.

Received for publication 20 August 1984 and in final form 14 December 1984.

REFERENCES

Auerbach, A., and F. Sachs. 1983. Flickering of a nicotonic ion channel to a subconductance state. *Biophys. J.* 42:1–10.

Auerbach, A., and F. Sachs. 1984. Single-channel currents from acetylcholine receptors in embryonic chick muscle. Kinetic and conductance properties of gaps within bursts. *Biophys. J.* 45:187–198.

Axelrod, D., A. Wright, W. Webb, and A. Horwitz. 1978. Influence of membrane lipids on acetycholine receptor and lipid probe diffusion in cultured myotube membrane. *Biochemistry.* 17:3604–3609.

Bendat, J. S., and A. G. Piersol. 1971. Random Data: Analysis and Measurement Procedures. Interscience Publishers, Inc., John Wiley & Sons, Inc., New York.

Careri, G., P. Fasella, and E. Gratton. 1975. Statistical time events in enzymes: a physical assessment. *Crit. Rev. Biochem.* 3, 141–164.

Colquhoun, D., E. Neher, H. Reuter, and C. F. Stevens. 1981. Inward current channels activated by intracellular Ca in cultured cardiac cells. *Nature (Lond.).* 294:752–754.

Colquhoun, D., and F. J. Sigworth. 1983. Fitting and statistical analysis of single-channel currents. *In* Single Channel Recording. E. Neher and B. Sakmann, editors. Plenum Publishing Corp., New York. 191–263.

Debrunner, P. G., and H. Frauenfelder. 1982. Dynamics of proteins. *Annu. Rev. Phys. Chem.* 33:283–299.

DeFelice, L. J. 1981. Introduction to Membrane Noise. Plenum Publishing Corp., New York.

Fahey, P. F., D. E. Koppel, L. S. Barak, D. E. Wolf, E. L. Elson and W. W. Webb. 1977. Lateral diffusion in planar lipid bilayers. *Science (Wash. DC).* 195:305–306.

FitzHugh, R. 1983. Statistical properties of the random asymmetric telegraph signal, with applications to single-channel analysis. *Math. Biosci.* 64:75–89.

Frehland, E., and K. H. Faulhaber. 1980. Nonequilibrium ion transport through pores. The influence of barrier structures on current fluctuations, transient phenomena and admittance. *Biophys. Struct. Mech.* 7:1–16.

Gurd, F. R. N., and T. M. Rothgeb. 1979. Motions in proteins. *Adv. Prot. Chem.* 33:73–165.

Hamill, O. P., A. Marty, E. Neher, B. Sakmann, and F. J. Sigworth. 1981. Improved patch-clamp techniques for high-resolution current recording from cells and cell-free membrane patches. *Pfluegers Arch. Eur. J. Physiol.* 391:85–100.

Hamill, O. P., and B. Sakmann. 1981. Multiple conductance states of single acetylcholine receptor channels in embryonic muscle cells. *Nature (Lond.).* 294:462–464.

Hooge, F. N. 1976. 1/f noise. *Physica.* 83B:14–23.

Horn, R., and M. S. Brodwick. 1980. Acetycholine-induced current in perfused rat myoballs. *J. Gen. Physiol.* 75:297–321.

Horn, R., and J. B. Patlak. 1980. Single channel currents from excised patches of muscle membrane. *Proc. Natl. Acad. Sci. USA.* 77:6930–6934.

Jackson, M. B., B. S. Wong, C. E. Morris, and H. Lecar. 1983. Successive openings of the same acetylcholine receptor channel are correlated in open time. *Biophys. J.* 42:109–114.

Karplus, M., and J. A. McCammon. 1981. The internal dynamics of globular proteins. *Crit. Rev. Biochem.* 9:293–349.

Läuger, P. 1975. Shot noise in ion channels. *Biochim. Biophys. Acta.* 413:1–10.

Magleby, K. L., J. N. Barrett, and B. S. Pallotta. 1982. Properties of single calcium-activated potassium channels in cultured rat muscle. *J. Physiol. (Lond.).* 331:211–230.

Marsh, D., A. Watts, R. D. Pates, and R. Uhl. 1982. ESR spin-label studies of lipid-protein interactions in membranes. *Biophys. J.* 37:265–274.

Marty, A. 1981. Ca-dependent K channels with large unitary conductance in chromaffin cell membranes. *Nature (Lond.).* 291:497–500.

McCammon, J. A., and M. Karplus. 1980. Dynamics of tyrosine ring rotations in a globular protein. *Biopolymers.* 19:1375–1405.

Neher, E., and C. F. Stevens. 1977. Conductance fluctuations and ionic pores in membranes. *Annu. Rev. Biophys. Bioeng.* 6:345–382.

Neumcke, B. 1978. 1/f noise in membranes. *Biophys. Struct. Mech.* 4:179–199.

Neumcke, B. 1982. Fluctuation of Na and K currents in excitable membranes. *Int. Rev. Neurobiol.* 23:35–66.

Rae, J. L., and R. A. Levis. 1984. Patch clamp recordings from the epithelium of the lens using glasses selected for low noise and improved sealing properties. *Biophys. J.* 45:144–146.

Sakmann, B., J. Patlak, and E. Neher. 1980. Single acetylcholine-activated channels show burst-kinetics in presence of desensitizing concentrations of agonist. *Nature (Lond.).* 286:71–73.

Sauve, R., and E. Bamberg. 1978. 1/f noise in black lipid membranes induced by ionic channels formed by chemically dimerized gramicidin A. *J. Membr. Biol.* 43:317–333.

Sigworth, F. J. 1982. Fluctuations in the current through open ACh-receptor channels. *Biophys. J.* 41(2, Pt. 2):47*a*. (Abstr.)

Sigworth, F. J. 1983. An example of analysis. *In* Single Channel Recording. E. Neher and B. Sakmann, editors. Plenum Publishing Corp., New York. 301–321.

Sine, S. M., and J. H. Steinbach. 1984. Agonists block currents through acetylcholine receptor channels. *Biophys. J.* 46:277–284.

Stevens, C. F. 1972. Inferences about membrane properties from electrical noise measurements. *Biophys. J.* 22:1028–1047.

Szabo, G. 1981. Internal gating of conductance in a gramicidin channel. *Biophys. J.* 33(2, Pt. 2):64*a*. (Abstr.)

Wagner, G., A. DeMarco, and K. Wüthrich. 1976. Dynamics of the aromatic amino acid residues in the globular conformation of the basic pancreatic trypsin inhibitor (BPTI). I. ^{1}H NMR studies. *Biophys. Struct. Mech.* 2:139–158.

Weissman, M. B. 1978. A mechanism for 1/f noise in diffusing membrane channels. *Biophys. J.* 21:87–91.

Yellen, G. 1982. Single Ca^{2+}-activated nonselective cation channels in neuroblastoma. *Nature (Lond.).* 296:357–359.

Yellen, G. 1984. Ionic permeation and blockade in Ca^{2+}-activated K^+ channels of bovine chromaffin cells. *J. Gen. Physiol.* 84:157–186.